

Bio-optical consequences of viral infection of phytoplankton: I. Experiments with the cyanobacterium, *Synechococcus* sp.

*W. M. Balch*¹

Bigelow Laboratory for Ocean Sciences, P.O. Box 475, W. Boothbay Harbor, Maine 04575

J. M. Vaughn

University of New England, Department of Microbiology, College of Osteopathic Medicine, University of New England, Biddeford, Maine 04005

J. I. Goes

Bigelow Laboratory for Ocean Sciences, P.O. Box 475, W. Boothbay Harbor, Maine 04575

J. F. Novotny

University of New England, Department of Microbiology, College of Osteopathic Medicine, University of New England, Biddeford, Maine 04005

D. T. Drapeau and E. S. Booth

Bigelow Laboratory for Ocean Sciences, P.O. Box 475, W. Boothbay Harbor, Maine 04575

*C. L. Vining*²

University of New England, Department of Microbiology, College of Osteopathic Medicine, University of New England, Biddeford, Maine 04005

Abstract

Four strains of the cyanobacteria, *Synechococcus*, were infected with viruses isolated and purified from coastal waters of the Gulf of Maine. Changes in host and virus concentration were observed in time course experiments, along with associated variability in inherent optical properties. There were strong optical shifts before and after lysis in inherent optical properties on time scales commensurate with the viral infection process. Specifically, both backscattering and absorption (particularly in visible wavelengths) increased slightly after infection, but decreased markedly after lysis. The most rapid optical change was seen in *in vivo* chlorophyll fluorescence, with a slight increase within 2 d after initial infection. Such changes likely reflect fundamental changes in host photophysiology after infection. After host lysis, there was a major drop in bulk Chl *a* fluorescence, synchronous with a major increase in the ratio of free viruses per host cell. The net effect of the changes in fluorescence and host concentration was an increase in the fluorescence per cell. These optical changes were accompanied by major changes in the submicron particle size spectra as cells were lysed, releasing their intracellular contents.

Viruses represent the most abundant form of life in the oceans (Paul et al. 1991), with concentrations typically ranging from 10² to 10⁸ mL⁻¹ in eutrophic regions (Bergh

et al. 1989; Suttle and Chan 1994). They were originally thought to be a potentially significant source of optical backscattering because of their high abundance (Morel and Ahn 1991; Stramski and Kiefer 1991). However, this notion was disproved after direct measurements of volume scattering of concentrated virus suspensions by Balch et al. (2000), who demonstrated that the low backscattering cross sections of viruses more than compensated their numerical abundance, and on their own, viruses had a negligible effect on optical backscattering in the marine environment.

Although viruses are optically insignificant, they do have a significant effect on their optically active hosts. For example, viral infection and lysis of heterotrophic bacteria were shown to dramatically change the shape of the volume-scattering function, making it flatter in both forward and backward directions (Balch et al. 2002). This effect was hypothesized to result from the conversion of the

¹ Corresponding author (bbalch@bigelow.org).

² Present address: Department of Marine Resources, P.O. Box 8, West Boothbay Harbor, Maine 04575-0008.

Acknowledgments

The authors thank W.H. Wilson and two anonymous reviewers who provided critical comments on an earlier draft of the paper. Primary support was generously provided by the Department of Environmental Optics, Office of Naval Research (grant N000014-05-1-0111). The National Aeronautics and Space Administration provided support through NASA EPSCOR (grant EP-02-14). Support was also provided by the National Science Foundation (OCE-0322074 subgrant S0993A-D; OCE-0325937). We thank Charles O'Kelly and Robert Andersen (Bigelow Laboratory for Ocean Sciences) for invaluable help with transmission electron microscopy. This is Bigelow Laboratory Contribution 200605.

Table 1. Definition and units of notation.

$a_{pg}(\lambda)$	Absorption of particulate and dissolved material at a given wavelength, λ (m^{-1})
$b_{b\ pg}(514)$	Backscattering of particulate and dissolved material at 514 nm (m^{-1})
CDOM	Chromophoric dissolved organic matter ($mg\ m^{-3}$)
Chl a	Chlorophyll a ($\mu g\ L^{-1}$)
d	Particle diameter (nm)
$D(\lambda)$	Optical density (unitless) at wavelength, λ defined as $\log_{10} I_0/I$, where I_0 is the light intensity incident on a material and I is the light intensity transmitted through a material
E_f	Efficiency of chlorophyll fluorescence ($F_{Chl\ a}(a_{pg}(440))$)
$F_{Chl\ a}$	Bulk fluorescence of Chl a (relative scale)
F_{cell}	Cellular Chl a fluorescence (relative scale)
λ	Wavelength of light (nm)
MOI	Multiplicity of infection (initial ratio of viruses per host at infection) (unitless)
FVPH	Ratio of free viruses per host cell after infection (unitless)
μ	Intrinsic rate of increase in abundance of host and viruses (d^{-1})

bacteria from particle scatterers (where their effective diameter, $d > \lambda$, the wavelength of light) to submicron particles dominated by molecular or Rayleigh scattering (where $\lambda > d$) (Mobley 1994). (Table 1 lists an explanation of this and all other notation used here.) Moreover, the lysis of the host bacteria resulted in the release of chromophoric dissolved organic matter (CDOM) with particle diameters $<0.2\ \mu m$ (Balch et al. 2002). Interestingly, after lysis, $0.45\text{-}\mu m$ -diameter particles formed over time, presumably as the newly released dissolved organic matter aggregated to form larger particles (Chin et al. 1998). This increase in aggregates dramatically increased the beam attenuation of the suspension (Balch et al. 2002).

To understand the effect of viruses on ocean optical properties, it is best to use a reductionist approach, focusing on the constituent absorption and backscattering properties of both viruses and their hosts (Morel and Ahn 1991; Stramski and Kiefer 1991). Micron- and submicron-sized particles are most important in determining particle backscattering (Morel and Ahn 1990) such that numerically abundant bacteria are important modulators of particle backscattering in the sea. Phytoplankton are of first-order importance in affecting both absorption and backscattering (Roesler and Perry 1989; Bricaud and Stramski 1990; Cleveland and Perry 1994). Virus-induced lysis of phytoplankton (particularly picophytoplankton), followed by CDOM release and aggregation, would be expected to affect the particle composition and packaging of cellular pigments and CDOM. This would also affect the slope of the particle size distribution (Twardowski et al. 2001), which in turn could have dramatic effects on backscattering, absorption, and, ultimately, reflectance (Gordon et al. 1988).

Little is known about the effects of viral infection on the absorption and scattering properties of photosynthetic organisms, or what optical changes follow lysis, and the time scales of these changes. Viral infection of *Synechococcus* (CCMP strain 1331) induced a dramatic ($>10\times$) decrease in optical volume scattering (and backscattering) but with minimal change in the shape of the volume scattering function (Balch et al. 2002; see their fig. 2D,H). This was unlike infection experiments with heterotrophic

bacteria, which showed strong changes in both the magnitude and the shape of the volume scattering function after viral infection (Balch et al. 2002). Optical changes (attributed to viruses) have been reported more recently in enclosed lake water experiments, in which the autotrophic assemblage was dominated by a filamentous cyanobacterial species, *Limnothrix* sp. (Simis et al. 2005). Scattering (estimated indirectly from the difference between attenuation and absorption) decreased 60–80%, and absorption decreased 20–80% after viral lysis. Their results clearly showed that natural lake populations of filamentous cyanobacteria could be susceptible to viral control, and that viral infection could have optical consequences on account of changes in water turbidity and absorption. Moreover, by making assumptions about the shape of the volume scattering function (Petzold 1972), Simis et al. (2005) concluded that remote-sensing reflectance might be expected to decrease after a mass lysis event. Direct measurements of volume scattering (and resultant backscattering) of infected host cells will help validate this result, especially given that three-quarters of the prokaryotic species examined previously showed strong changes in the shape of the volume scattering function after infection (Balch et al. 2002).

Autofluorescence (inelastic scattering) of photosynthetic eukaryotes likely will change after viral infection because the integrity of the chloroplast-containing cells is destroyed, thus disrupting the energy transfer between the light-capturing photosystems and the dark reactions of photosynthesis (Seaton et al. 1995; Juneau et al. 2003). Chlorophyll fluorescence has been used as an indicator of infectivity for *Chlorella* virus (Rohozinski et al. 1995). Virus additions to eutrophic and oligotrophic phytoplankton caused changes in in vivo chlorophyll fluorescence (Hewson et al. 2001).

Most previous optical experiments involving viruses have dealt with their effects on bacterial scattering, mainly because of the numerical abundance of bacteria and bacteriophage in the sea, and the important contribution of bacteria to total backscattering (Morel and Ahn 1990). However, photosynthetic organisms can also be abundant in the sea, and they demonstrate strong scattering plus

absorption (as a result of the presence of photosynthetic and photoprotective pigments). Here we describe the effects of viral infection on several strains of the prokaryotic cyanobacteria, *Synechococcus* sp., and the ensuing optical changes in host elastic scattering, chlorophyll *a* (Chl *a*) fluorescence (inelastic scattering) and spectral absorption. *Synechococcus* is responsible for a significant fraction of ocean primary production, especially in tropical and temperate waters (Goericke and Welschmeyer 1993). It harvests photons with phycobilisomes, cellular structures that contain pigment-protein complexes that have the accessory pigment phycoerythrin. There are two types of chromophore pigment-protein complexes in *Synechococcus*, phycourobilin (495-nm peak absorption in vivo) and phycoerythrobilin (545-nm peak absorption in vivo) (Ong and Glazer 1991). These pigments, along with Chl *a*, represent the major absorbing pigments of *Synechococcus* sp. in the visible wavelengths. Variable ratios of these pigments have been thought to be an indicator of oceanic versus coastal strains of *Synechococcus* sp. and adaptations to improving light harvesting in variable spectral water types (Wood et al. 1998). However, more recent molecular evidence contradicts this notion (Toledo et al. 1999).

Another interesting aspect of *Synechococcus* is that its genome has been strongly affected by horizontal gene transfer via phages (Palenik et al. 2003), an excellent indicator that viruses exert considerable selective pressure on the cyanobacteria in nature (Suttle and Chan 1993). In the field, cyanophage concentrations are 10–100× less abundant than their hosts (Wilson et al. 1993). Indeed, changes in virus abundance in the field seem to be more related to the abundance of *Synechococcus*, rather than heterotrophic bacteria (Bettarel et al. 2002). Waterbury and Valois (1993) hypothesized that *Synechococcus* populations are dominated by strains that are resistant to cyanophages present in seawater. Moreover, they suggest that these phages are maintained in the natural microbial assemblage by infecting relatively rare, non-resistant cells. By means of plaque assay studies, Wilson et al. (1996) demonstrated that infected *Synechococcus* strain 7803 showed lysogeny under phosphorous-deplete conditions, but the infections became lytic under phosphate-replete conditions. Lysogeny has also been shown to occur seasonally in natural populations of *Synechococcus*, which would confer immunity from other viral attacks (McDaniel et al. 2002).

Below, we describe a series of experiments on the optical effects of viral infection of *Synechococcus*. The first step was to isolate and purify viruses that were capable of lysing host *Synechococcus* clones. Transmission electron microscopy was used to confirm the types of viruses as well as the infection process. The experimental design involved adding a known titer of viruses to replicate cultures of *Synechococcus* cells (replicate flasks without viruses served as uninfected controls). Over time, the concentration of hosts and viruses were measured, along with changes to volume scattering and spectral absorption. We also documented the changes in in vivo Chl *a* fluorescence resulting from viral infection and estimated changes in the fluorescence efficiency as infection proceeded.

Methods

Propagation of host cells—Cultures of *Synechococcus* sp. used in these experiments were obtained from the Bigelow Laboratory Center for the Collection of Marine Phytoplankton (CCMP). The strains included CCMP 1333 (*Synechococcus bacillarus* Butcher; also known as “SYN”; axenic), CCMP 1334 (*Synechococcus* sp.; also known as “WH7803” and “DC-2”; axenic), CCMP 835 (*Synechococcus* sp.; also known as “6B3SYN”; nonaxenic) and CCMP 833 (*Synechococcus* sp.; also known as “SYN48,” “WH6501”). Although the latter two strains were technically nonaxenic, they only contained small numbers of heterotrophic bacteria that became apparent late during the experiment. Strains CCMP 1333 and 1334 were propagated in *f/2* medium at 26°C with low-speed rotary shaking under low-light conditions ($\sim 8 \mu\text{mol m}^{-2}\text{s}^{-1}$), on a 14 h light:10 h dark cycle. Strains 833 and 835 were also propagated on *f/2* medium in batch culture at 26°C (833) and 17°C (835), respectively, under similar light conditions. On the day of an experiment, cultures were diluted 1:2 with fresh, sterile media. The temperature in the incubator was maintained at 26°C for experiments with CCMP 1333 and 1334, 24°C for CCMP 833, and 17°C for CCMP 835, and light conditions were identical to those already described.

Viruses—Viruses specific for *Synechococcus* strains CCMP 1333, 1334, and 833 were isolated from the waters of West Boothbay Harbor. Viruses infecting the CCMP 835 strain of *Synechococcus* were isolated from the waters of the Gulf of Maine (43°44.39 N, 67°07.98 W). Isolations involved a modification of the enrichment method previously described by Balch et al. (2000). Briefly, 600-mL cultures of exponentially growing host cells, propagated as described above, were centrifuged ($4,000 \times g/15 \text{ min}$) and resuspended in 20 mL *f/2* medium. Five-milliliter aliquots of this concentrate were inoculated either into triplicate flasks containing 100 mL of triple-strength *f/2* medium mixed with 200 mL filtered (0.45 μm) seawater sample, or into a control flask containing 300 mL *f/2*. All flasks were incubated as above for 5–6 d and inspected daily for clearing consistent with host lysis. Cultures showing host lysis were filtered through 2% fetal calf serum-treated 0.2- μm filters and inoculated into fresh host cultures. Resulting lysates were filtered once again through 0.2- μm porosity filters and samples stained with SYBR Green for the presence of virus-like particles (Noble and Fuhrman 1998). Putative virus isolates underwent a 2× extinction dilution (Cottrell and Suttle 1991) and were purified by cesium chloride density gradient ultracentrifugation (Balch et al. 2000). Morphological studies of purified isolates were conducted by transmission electron microscopy procedures reported previously (Balch et al. 2002).

Experimental manipulation—Each experiment was begun with one host culture diluted 1:2 with fresh *f/2* media to a total volume of 2 liters, which was then divided equally among four flasks, two experimental and two control flasks (host concentration $\sim 10^6$ to 10^7 mL^{-1}). Control flasks received no virus inocula, whereas the experimental flasks

received 2 mL of purified, concentrated virus stock (titers of 5×10^6 to 1×10^7 mL⁻¹), yielding an approximate multiplicity of infection (MOI) of 1. After a zero-time sample, each flask was sampled daily at approximately the same time for virus and host enumeration plus optical properties.

Enumeration of virus and host—Free virus enumeration was performed daily following the SYBR Green method (Noble and Fuhrman 1998), followed by direct microscopic virus counts with an Olympus BH2 or BX-51 microscope equipped with epifluorescence capabilities. Host *Synechococcus* enumerations were performed by counting auto-fluorescent cyanobacterial cells that were retained on a 0.02- μ m filter (Whatman). Hosts were also enumerated in the SYBR Green counts. Comparison between the SYBR Green and autofluorescence counts helped confirm that the contaminating bacteria in the two nonaxenic strains were several orders of magnitude less abundant than the *Synechococcus* sp. At least 200 particles were counted for each virus or host enumeration.

Flow-field fractionation—Flow, field-flow fractionation (FFFF) measurements were used to measure the size spectrum of submicron particles (including viruses). This is a technique used in our previous virus studies to characterize virus size and the size spectrum of exudates released after viral lysis of hosts (Vaillancourt and Balch 2000; Balch et al. 2002).

Optical measurements—For each sample, three optical properties were measured: volume scattering at 514 nm, chlorophyll fluorescence, and spectral absorption. Absorption was measured with a Camspec spectrophotometer equipped with an integrating sphere. A 1-cm quartz cuvette with liquid sample was placed at the beam entrance of the integrating sphere port. A cell blank of filtered (0.02 μ m) Milli-Q purified water was used. The optical thickness of the cuvette was kept low in order to avoid multiple scattering. Scans of optical density, $D(\lambda)$, were made between 200 and 800 nm with a 1-nm slit width. Absorption coefficients, $a(\lambda)$, were calculated as

$$a(\lambda) = 2.303[D(\lambda) - D(800)]/r \quad (1)$$

where the factor 2.303 converts from log₁₀ to log_e, and r is the cuvette optical path length (cm). A scattering correction was made by subtracting the value at 800 nm from the spectral optical density values. This correction typically was minimal because we used an integrating sphere that already accounted for most of the scattered light.

Optical effects of viral infection on optical scattering were examined with a Wyatt Technologies Dawn-F light-scattering photometer equipped with an argon-ion laser (Balch et al. 1999; Balch et al. 2002). We measured the scattering phase function at a rate of 200 Hz for 10 s (i.e., $n = 2,000$ for each measurement). Five replicate measurements were made on each sample. The sensed volume in the instrument was 250 μ L. This instrument measured the volume scattering function (at 514 nm) at 15 angles; the

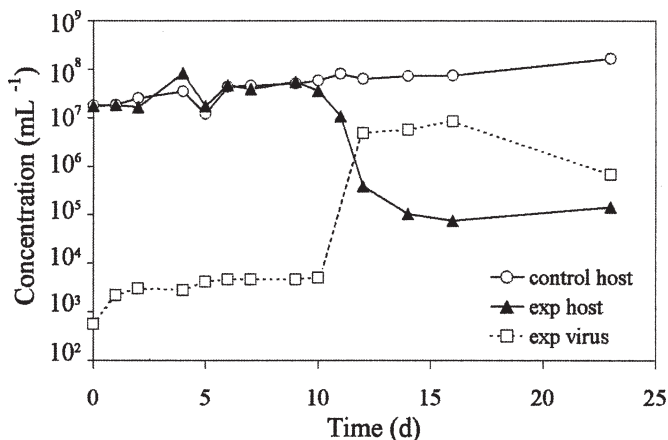


Fig. 1. Typical time course of viral and bacterial abundance in control and experimental flasks, for infection experiment three (Table 2) with *Synechococcus* strain 1334.

backscattering coefficient for particulate and dissolved material ($b_{b, pg}$) was calculated by fitting a Beardsley Zaneveld function (Beardsley and Zaneveld 1969; Gordon 1976) to the 15 angles of volume scattering, then integrating this function over the backward angles to calculate backscattering. Such estimates are within 5% of those based on trapezoidal integration (Balch et al. 1999; Balch and Drapeau 2004). Blanks were run with ultrafiltered 0.02- μ m-filtered Milli-Q water and subtracted from the measured values to estimate the backscattering due to particulate and dissolved materials.

In vivo Chl a fluorescence ($F_{Chl a}$) of host cells was measured daily with a Turner Designs 10AU-005-CE fluorometer equipped with the sample tube holder. The fluorometer used a daylight white F4T5D lamp, blue-violet excitation filter (peak excitation 438 nm with half-band pass of 340–500 nm), and red emission filter (high pass >665-nm interference filter).

Results

Typical host and virus abundance time course experiments had the patterns shown in Fig. 1, an experiment performed with *Synechococcus* strain 1334 (experiment 3, Table 2). Uninfected control *Synechococcus* showed log linear increases in abundance, whereas infected *Synechococcus* numbers paralleled the changes in the control flask until about day 10, after which they dropped sharply ($\sim 1,000\times$ on day 11), followed by slight increases for the next 2 weeks. Trends of virus abundance were roughly opposite to the trends of the host. That is, numbers stayed low for about 10 d, after which there was an increase of $1,000\times$ in concentration on day 11, followed by a decline over the next 2 weeks. Table 2 summarizes the results of seven 2–4-week *Synechococcus* sp. infection experiments (performed with the *Synechococcus* sp. strains mentioned above). Specific rates of change were determined from slopes of the abundance data derived from semilog plots of abundance (particles mL⁻¹) versus time (d). The uninfected control flasks showed logarithmic host growth rates of 0.1–0.7 d⁻¹, sometimes after a short lag phase (e.g., experiment

Table 2. Details about experiments, clones, host growth rates, and virus propagation rates, length of time (d) to viral burst in abundance, culture clearing, change in Chl *a* fluorescence, peak virus abundance, and peak concentrations of virus. Rates of increase of hosts and viruses are provided for three phases of each experiment: "initial," immediately after infection but before major viral burst; "middle," when major increases in virus abundance were noted; and "late," after a major host lysis event, during period of subsequent growth of virus-resistant host cells.

Exp. no.	Length (d)	Host clone	Host growth rates, μ (d ⁻¹)						Virus propagation, μ (d ⁻¹)								
			Control			Experimental			Experimental			Experimental					
			Initial	Middle	Late	Initial	Middle	Late	Initial	Middle	Late	Initial	Middle	Late			
1	32	Syn 1333	0.60	0.12	0.01	0.44	-0.02	-0.02	-0.02	0.22	0.73	-0.06	5	5	2	11	3.2 × 10 ⁷
2	27	Syn 1333	0.05	0.33	0.05	0.16	-0.42	0.18	0.73	1.61	0.73	0	5	3	6	23	1.0 × 10 ⁸
3	23	Syn 1334	0.10	0.10	0.10	0.13	-2.27	0.09	3.44	0.14	0.14	10	11	10	10	16	7.0 × 10 ⁶
4	19	Syn 1334	0.31	0.31	0.00	0.32	-1.91	0.45	4.08	0.28	0.28	6	10	7	10	19	3.0 × 10 ⁶
5	20	Syn 835	0.74	0.16	-0.03	-1.11	-0.32	0.19	2.79	0.72	-0.13	0	10	4	4	8	1.5 × 10 ⁹
6	24	Syn 835	0.46	0.46	-0.06	0.60	-0.12	0.18	2.02	-0.29	-0.29	2	No clearing	2	6	8	2.8 × 10 ⁹
7	13	Syn 833	0.16	0.01	-0.28	-0.56	-0.26	-1.68	0.86	-0.20	1.48	0	5	5	1	5	6.0 × 10 ⁶

2). With the exception of experiment 3, the cells reached stationary phase later in the experiment, with cessation (or slight declines) in growth rate ($\mu = 0.05$ to -0.28 d⁻¹). In contrast, infected host cells generally showed significant declines in abundance in the early to middle parts of the experiment, shortly after infection (-0.56 to -2.27 d⁻¹). The timing of the host decrease varied with host and virus strains, but in all cases, the decrease in hosts in the experimental "infected" flask occurred well before the control culture reached stationary phase (which often occurred ~3 weeks later). This indicated that the experimental effects observed here were not due to nutrient limitation.

Virus abundance in the experimental flask showed significant increases before or concurrent with the collapse of the host abundances. The infection of *Synechococcus* strain 1334 showed virus increases at roughly twice the rate of the host mortality rate (3.44 to 4.08 d⁻¹ vs. -1.91 to -2.27 d⁻¹ for virus and host, respectively). It was also evident that toward the end of the experiments, virus replication slowed or slightly declined (with the exception of experiment 7; Table 2). Table 2 also summarizes the timescales of the burst in virus replication after infection (0–10 d), culture clearing (5–11 d), effects on bulk auto-fluorescence ($F_{Chl a}$; 1–10 d), and peak virus concentration (5–23 d). Interestingly, the typical sequence of viral infection was as follows: (1) rapid virus replication, (2) changes in $F_{Chl a}$, (3) culture clearing, and (4) peak virus concentration. In all cases, these were not single-step growth experiments, but in all likelihood involved multiple infection cycles, especially given the length of the experiments. Thus, relating the intrinsic rate of decrease of host to the simultaneous propagation rate of viruses should be done cautiously, especially early in the experiments, when virus and host abundances were low, when the likelihood of counting errors was greater.

Transmission electron micrographs of *Synechococcus* CCMP 1333 virus and *Synechococcus* CCMP 835 virus are shown in Fig. 2A and 2B, respectively. The CCMP 1333 viruses appeared to have an icosahedral head with a diameter of ~40 nm, and some tails were evident (Fig. 2A, arrow). The CCMP 835 viruses had icosahedral heads that were 50 nm in diameter, with distinct 100-nm noncontractile, straight tails (siphonophages; Fig. 2B). No evidence of a tapered collar was evident, as reported previously by Wilson et al. (1993).

Results from the FFFF demonstrated that the sub-micron particle size distribution were almost identical at 5 and 9 d after infection, with peaks at about 500 nm (Fig. 3). By day 13, the 500-nm peak in the infected flask was reduced to a third of the control, and a smaller peak was evident between 125 and 200 nm. By day 16, the largest peak in the infected flask was at ~300 nm (compared to the 450-nm peak in the control). Moreover, the small peak at 150–200 nm was still visible. By day 23, there appeared to be measurable 400–500-nm particles in both control and infected flasks, as well as a minimum in the particle size distribution at 250 nm. We also noted increased numbers of 500–1,000-nm particles in the infected flask.

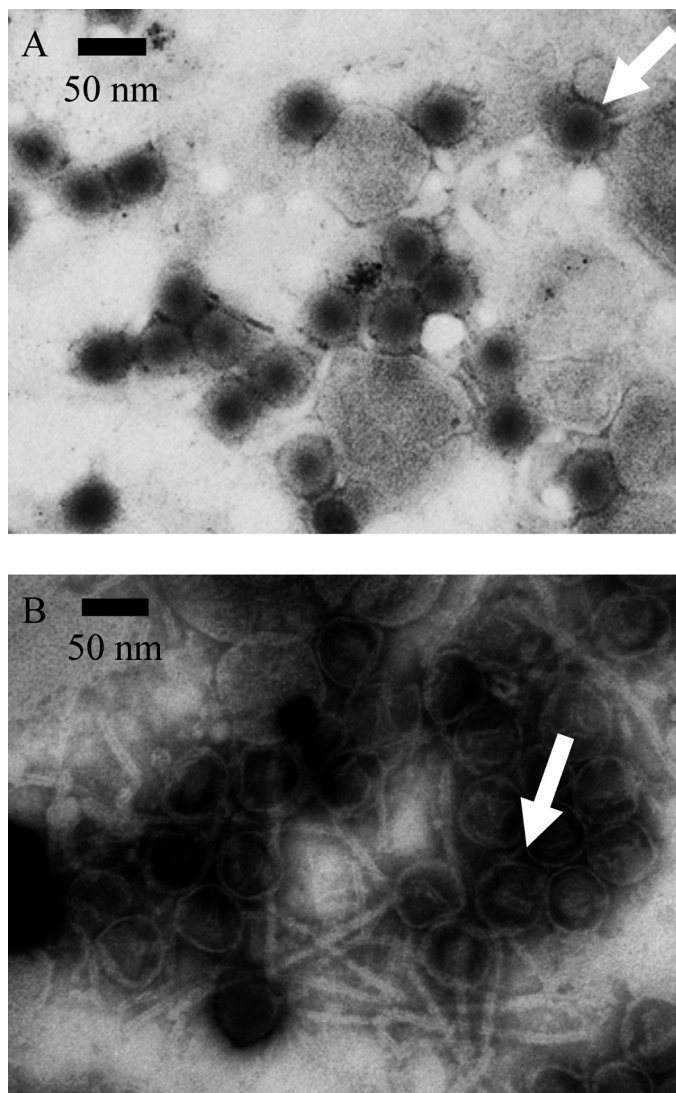


Fig. 2. Transmission electron micrographs of two of the viruses isolated in this study. (A) *Synechococcus* CCMP 1333 virus. Arrow points to virus particle with capsid of ~ 40 nm and evidence of tail. (B) *Synechococcus* CCMP 835 virus. Arrow points to single virus with 50 nm diameter, icosahedral capsid. Numerous viruses with 100 nm noncontractile, straight tails can be seen. Scale bar in each micrograph is 50 nm.

Optical results—Backscattering trends in most infection experiments showed that the infected cells lost backscattering at a rate of 0.1 to 0.8 d^{-1} (Table 3). In experiment 6, there was no change in $b_{b_{pg514}}$, whereas in experiment 7, the $b_{b_{pg514}}$ of infected cells increased, but at about one-fourth of the increase in the control flask (Table 3). The pattern of backscattering loss consistently showed similar patterns with a strong decrease relative to the control several days after infection. For the *Synechococcus* CCMP 1334 infection experiment in Fig. 1, there was a 3 \times decrease in particle backscattering at 514 nm, which began 10–11 d after infection and occurred at a rate of -0.66 d^{-1} (Fig. 4A). In contrast, backscattering in the control flask increased at a relatively slow rate of $\sim 0.08 \text{ d}^{-1}$ during the

entire experiment. It is worth noting that total particle backscattering of the infected experimental flasks often was slightly higher after day 1 and remained that way until the culture cleared (Fig. 4A). Moreover, after the culture clearing, a slight increase in $b_{b_{pg}}(514)$ of 0.06 to 0.08 m^{-1} was evident in the virus-infected flask. This was seen in most experiments.

Absorption at 440 nm (Soret absorption band of Chl *a*) also showed a dramatic decrease between days 10 and 12 after infection at a rate of -0.62 d^{-1} , as compared to the monotonic increase in 440 nm absorption of 0.1 d^{-1} in the uninfected control flask (Fig. 4B). We also observed that absorption in the infected flask, although identical to the control flask at time 0, was consistently $\sim 1 \text{ m}^{-1}$ greater than the control flask between days 1 and 9 (recall a similar trend in the particulate backscattering results; Fig. 4). Absorption changes due to infection were not identical at all wavelengths, however. Specific rates of change of absorption were most pronounced at 630 nm, an absorption peak of phycocyanin (Kirk 1994) (Fig. 5). Pronounced decreases in absorption were also observed at 440 nm (Chl *a*) and 543 nm (phycoerythrin). Absorption in the control flask increased monotonically for all wavelengths except 219 nm (216 nm is the absorption peak of nitrate; Ogura and Hanya 1967), which decreased gradually over the experiment as nitrate was consumed by the *Synechococcus*. In most experiments, this pattern was reproduced, with absorption of infected host cells showing significant decreases relative to the control cells at all wavelengths except in the ultraviolet (UV) (Table 3).

As might be expected from Fig. 5, spectral absorption began changing on day 11 and was markedly different by day 12 in the experimental flask (Fig. 6). In the control flask, the absorption above ~ 250 nm increased with host growth over each day of the experiment. In the infected experimental flask, absorption features began to disappear above 400 nm, relative to the control, after day 9. By day 12, the 680-nm absorption peak was reduced to levels originally seen on day 4, and by day 16, almost all detail in the absorption spectrum was gone except for a gradual spectral decrease in absorption across the spectrum, from the UV to the red. At the blue end of the spectrum, a slight rebound of absorption was evident on day 14 (data not shown) and day 16 relative to day 12 as virus-resistant cyanobacteria began to grow again (Fig. 1).

Fluorescence intensities of infected cells showed strong decreases relative to the fluorescence in the control flasks in all experiments (Table 3). For the same *Synechococcus* CCMP 1334 infection experiment shown in Fig. 1, $F_{\text{Chl } a}$ was always slightly higher in the infected flask than in the control flask between days 1 and 9. After this time, $F_{\text{Chl } a}$ dropped $>10\times$ from days 10 to 16 (Fig. 7), whereas the $F_{\text{Chl } a}$ values in the control flask increased another 50% during the same time period. The relative efficiency of red chlorophyll fluorescence was estimated as

$$E_{fl} = F_{\text{Chl } a}(a_{pg}(440)) \quad (2)$$

This definition assumes that $a_{pg}(440)$ is driven by Chl *a*, but it is known that dissolved organic matter also absorbs in

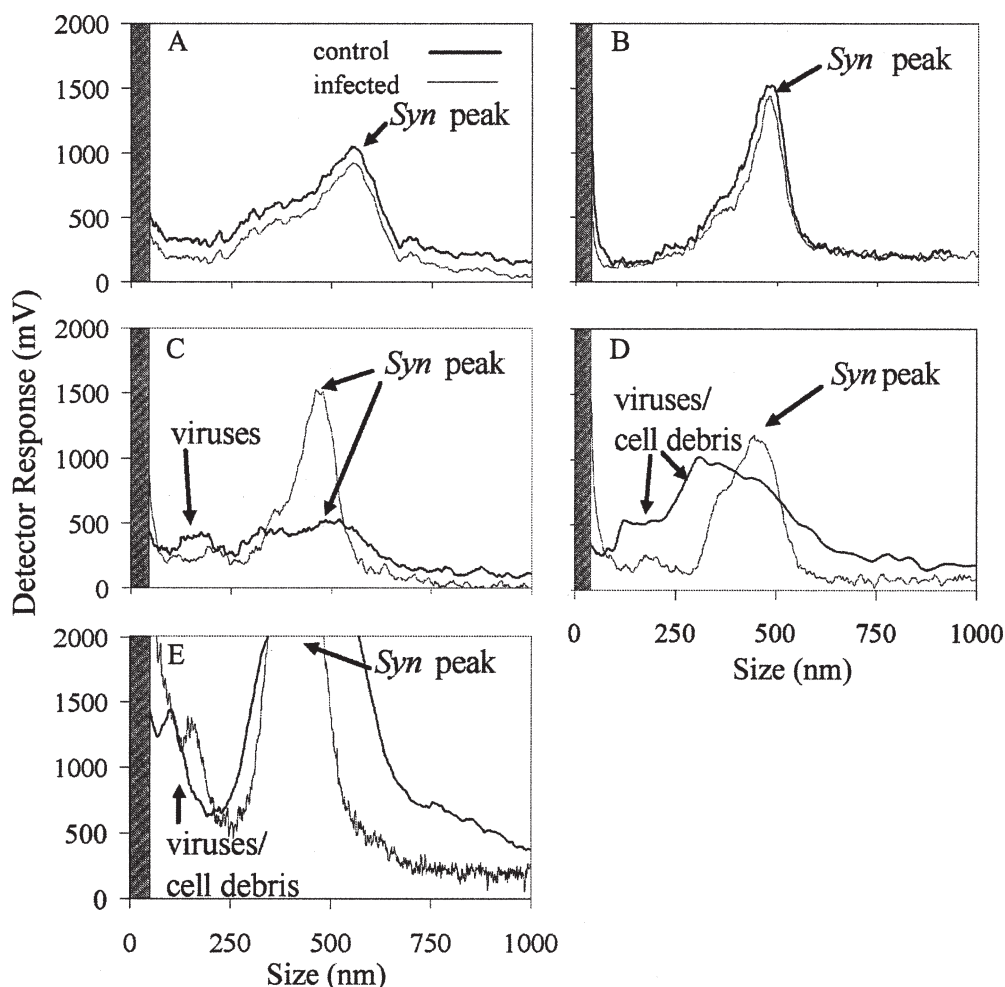


Fig. 3. Flow field flow fractionator results for same infection experiment with *Synechococcus* strain 1334 described in Fig. 1. Selected fractograms are shown for five time points after infection: (A) 5 d, (B) 9 d, (C) 13 d, (D) 16 d, and (E) 23 d. Thin black line represents uninfected control, heavier black line represents infected experimental flask. Note for sizes <50 nm (area obscured by bars at left of each panel), particles >1,000 nm also can be found in this fraction because of the physics of the particle elution (*see text*), and the size determination is not reliable.

this waveband. Thus, the relative efficiencies estimated here should be interpreted as conservative minimum values. Values of E_{fl} remained constant or increased in both control and experimental flasks until day 12, after which the efficiency in the experimental flask declined until day 16 (Fig. 7B). Relative chlorophyll fluorescence per host cell (F_{cell}) was roughly the same in the control and experimental flasks until day 9, after which F_{cell} increased almost 50 \times higher than control values by day 12 and stabilized at a value $\sim 100\times$ higher until the end of the experiment (Fig. 7C). Trends in F_{cell} for infected *Synechococcus* cells paralleled the trends in the ratio of free viruses per host cell (FVPH), and F_{cell} values increased typically 10–100 \times over the uninfected cells in all but experiment 1 (Table 3).

Discussion

The timescales of *Synechococcus* infection and optical changes were not the same in each experiment, with cultures clearing over periods of 5 to 11 d after infection.

One of the few previous studies where an optical change was quantified after viral infection of *Synechococcus* (strain 1334) was the study of Wilson et al. (1996) (*see their figs. 3 and 4*). They reported time series measurements of *Synechococcus* absorbance at 750 nm after addition of a cyanophage, S-PM2, isolated from the waters off Plymouth, U.K. A comparison of their results with ours is useful, but this needs to be done with caution because they did not use an integrating sphere spectrophotometer in their measurements (W. Wilson pers. comm.). Thus, the near-infrared extinction that they reported was likely dominated by scattering and not absorbance (because the ratio of scattering to absorption is highly increased in the near infrared; Babin and Stramski 2002). Thus, their results likely represent total scattering, whereas ours specifically quantified light scattering in the backward direction; these two variables might not be expected to respond identically before and after lysis. Indeed, the timescales of the decline in *Synechococcus* light scattering reported by Wilson (1996) were 1–2 d after infection, faster than the 5–11-d time

Table 3. Specific rates of change (d^{-1}) of backscattering (514 nm), absorption (270, 440, 496, 514, 547, 630, and 680 nm), and bulk Chl a fluorescence, $F_{Chl\ a}$ (d^{-1}) in control (uninfected) and experimental (Exp.; infected) flasks, respectively. Rightmost two columns give the relative cellular Chl a fluorescence in control (uninfected) and experimental (infected) flasks, respectively. Results are given from the middle portion of each infection experiment associated with increases in virus abundance and mortality of host cells.

Exp. No.	Rate of change of $b_{pg}(514)$ (d^{-1})		Specific rate of change of $a_{pg}(\lambda)$ (d^{-1})												Rate of change of $F_{Chl\ a}$ (d^{-1})		Relative chlorophyll fluorescence (cell $^{-1}$)			
			270 nm		440 nm		496 nm		514 nm		547 nm		630 nm		680 nm					
	Control	Exp.	Control	Exp.	Control	Exp.	Control	Exp.	Control	Exp.	Control	Exp.	Control	Exp.	Control	Exp.	Control	Exp.	Control	Exp.
1	0.098	-0.087	0.105	0.049	0.118	-0.048	0.107	-0.034	0.105	-0.043	0.123	-0.040	0.093	-0.018	0.115	-0.027	0.120	-0.173	2.6×10^{-7}	2.0×10^{-8}
2	0.093	-0.108	0.139	0.000	0.129	-0.201	0.075	-0.176	0.080	-0.379	0.273	-0.374	0.109	-0.363	0.124	-0.309	0.085	-0.048	5.0×10^{-7}	6.0×10^{-5}
3	0.080	-0.658	0.091	0.075	0.098	-0.622	0.105	-0.567	0.141	-0.277	0.124	-0.897	0.110	-1.382	0.116	-0.507	0.005	-0.434	1.5×10^{-7}	1.4×10^{-5}
4	0.112	-0.767	0.292	-0.161	0.452	-0.691	0.351	-0.239	0.175	-0.785	0.351	-0.279	0.234	-0.896	0.365	-0.376	0.171	-0.699	1.8×10^{-7}	1.0×10^{-5}
5	0.058	-0.127	0.079	0.054	0.212	-0.306	0.212	-0.531	0.200	-0.402	0.222	-0.433	0.276	-0.404	0.212	-0.531	0.026	-0.075	1.0×10^{-7}	2.0×10^{-5}
6	0.047	0.047	0.548	0.088	0.436	0.151	0.658	0.074	0.326	0.168	0.401	0.142	1.230	0.046	1.230	0.130	0.138	-0.190	3.0×10^{-8}	5.0×10^{-7}
7	0.175	0.046	-0.066	-0.201	0.287	0.067	0.457	0.287	0.130	0.000	0.338	0.237	0.276	0.132	0.358	0.181	0.065	-0.545	6.0×10^{-7}	3.5×10^{-6}

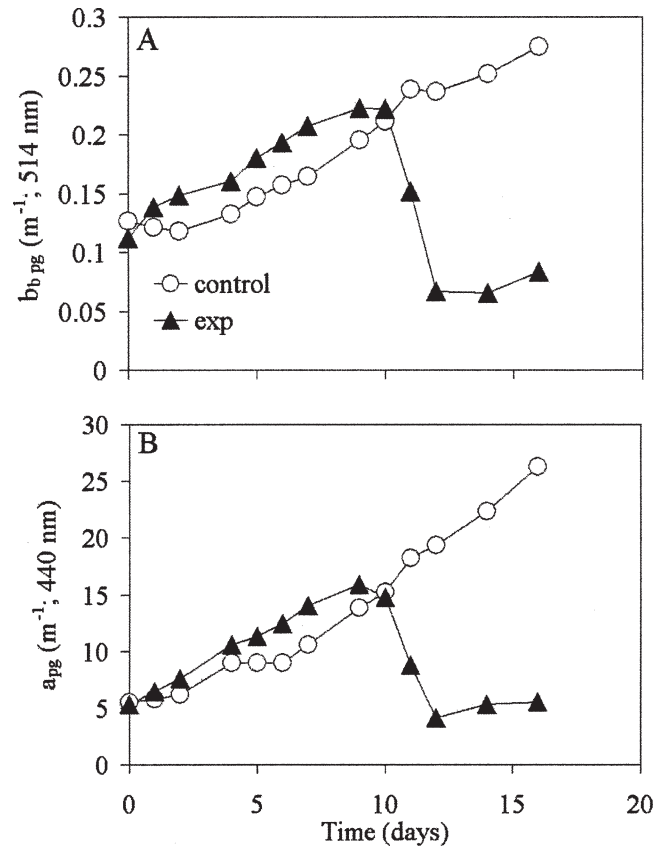


Fig. 4. (A) Time course of $b_{pg}(514)$ (m^{-1}) during viral infection experiment with *Synechococcus* strain 1334 (same experiment as in Fig. 1). (B) Time course of $a_{pg}(440)$ (m^{-1}) during infection experiment of *Synechococcus* strain 1334.

period that we observed between initial infection and a decline in backscattering. The most likely reasons for the temporal differences in optical changes for the Wilson et al. (1996) study and ours were differences in host growth conditions (e.g., media nutrient concentrations, temperature, light levels, and photoperiod) or differences in the strains of the viruses used.

Even with this temporal variability in infection kinetics, a strong covariation was evident between the extent of infection and the optic properties. Time scales of virus increases were similar to the time scales of variability in culture scattering, absorption, or fluorescence, which strongly implies a cause-and-effect relationship (Tables 2 and 3). A closer examination of the data also revealed a distinct sequence of events in the infected flasks. A decrease in fluorescence occurred on or before the time of host lysis, which preceded culture clearing. This might be expected given that the decrease in bulk fluorescence represents either a change in the chlorophyll concentration per cell, or a change in the physiological state of the cells. The latter is especially likely, given that fluorescence is tied to cellular processes such as photosynthetic electron transport, which would be affected during lysis when cell membranes are breached, causing leakage and breakdown of chemical gradients.

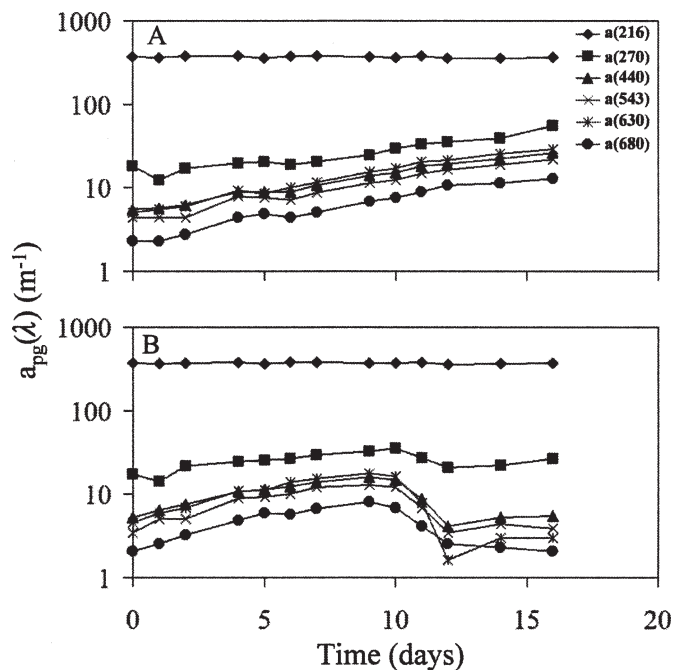


Fig. 5. Time course of a_{pg} (m^{-1}) at six wavelengths for viral infection of *Synechococcus* strain 1334 (same experiment as in Fig. 1). All absorption values have been corrected for scattering at 800 nm. (A) Uninfected control flask. (B) Infected experimental flask.

The time course of virus abundance in the infected flasks showed a distinct pattern too. Before culture lysis, for about 10 d, daily virus counts increased slowly and monotonically, typically at rates close to the growth rate of the host (Fig. 1, Table 2). However, virus-sized particles were not visible in the FFFF fractograms during this early stage of the infection (Fig. 3A,B), possibly as a result of the signal being too low for the FFFF. After the main lytic event, however, there was a strong difference in the fractogram particle size distributions as host cells were destroyed and cellular debris produced (e.g., disappearance of the 400–500-nm-sized peak and appearance of smaller particles; Fig. 3C). Optical changes at this point were significant, with major losses of backscattering (Fig. 4A), major decreases in absorption in the visible bands, with less relative decrease in absorption noted in the UV. (Figs. 4–6). The reason for this disparity between the absorption in the visible and UV is not immediately obvious. Proteins and nucleic acids probably were responsible for the bulk of particle absorption in the UV, regardless of whether the cells were lysed. Viral nucleic acids also absorb in the UV spectrum, which would have contributed to the bulk UV absorption in the infected host suspension. Note particularly how in the full spectral view (Fig. 6), relative changes in shape of the absorption spectrum were subtle in the UV. In contrast, pigment–protein complexes, which absorb in the visible spectrum, may have been subject to more photo-oxidation and breakdown when they were released from cells. This was readily apparent in Figs. 5 and 6, which show rapid decreases in absorption at 440 nm (Chl *a* peak), 495 nm (phycouribilin peak), and 543 nm (phycocyanin absorption peak).

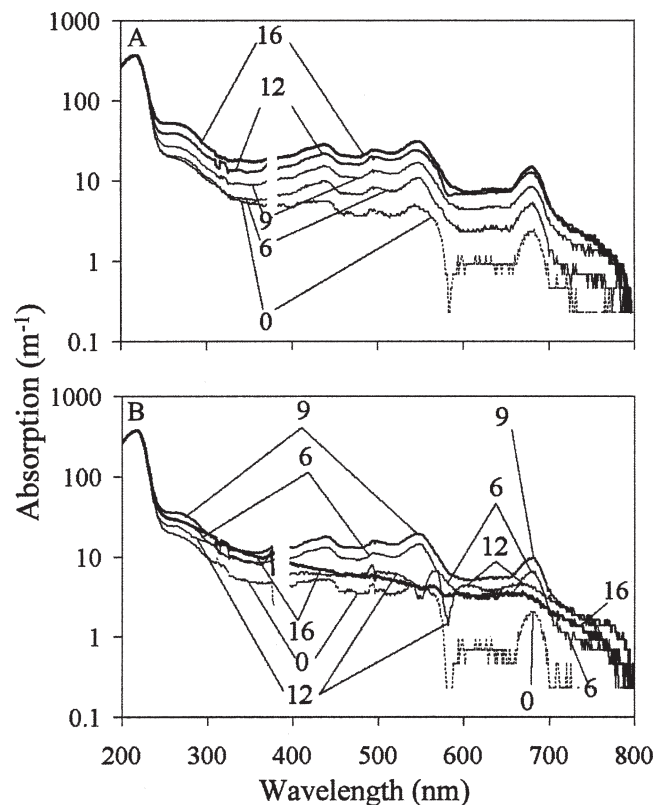


Fig. 6. Absorption spectra (a_{pg} ; m^{-1} ; scattering corrected) from 200 to 800 nm for control and experimental flasks during infection experiment with *Synechococcus* strain 1334 (same experiment as in Fig. 1). Number designations associated with each curve refer to the days after infection. Time zero spectra indicated with dashed line; all other spectra indicated with solid lines, with thickness of connecting lines increasing with culture age. (A) Uninfected control flask. (B) Infected experimental flask.

bilin peak), with the most rapid decrease in absorption at 630 nm (phycocyanin absorption peak).

One of the most striking optical changes that we observed during the infection process was an increase of $F_{Chl a}$, 24 h after infection, then a subsequent decrease in $F_{Chl a}$ just before lysis with almost complete loss of $F_{Chl a}$ after the peak in virus abundance. Interestingly, in the early phase of infection, while fluorescence was actually increasing, the number of host cells in control and infected flasks were about the same (Figs. 1 and 7A), and there was no detectable difference in the particle size distribution between control and experimental flasks (Fig. 3A,B). Thus, the fluorescence change during this time did not result from a greater abundance of host cells. However, backscattering and absorption were increased in experimental flasks (Fig. 4A,B), suggesting physiological changes, such as enhanced pigment synthesis and accumulation within the cells (which would have increased the 440-nm absorbance; Fig. 4B). As noted above, the increase in backscattering was not due to a change in cell size (Fig. 3); thus, it must have been due to intracellular optical changes (e.g., changes in refractive index).

A plot of $F_{Chl a}$ versus $a_{pg}(440)$ (the slope of which is E_{Π} given in Fig. 7B) showed that the time course of

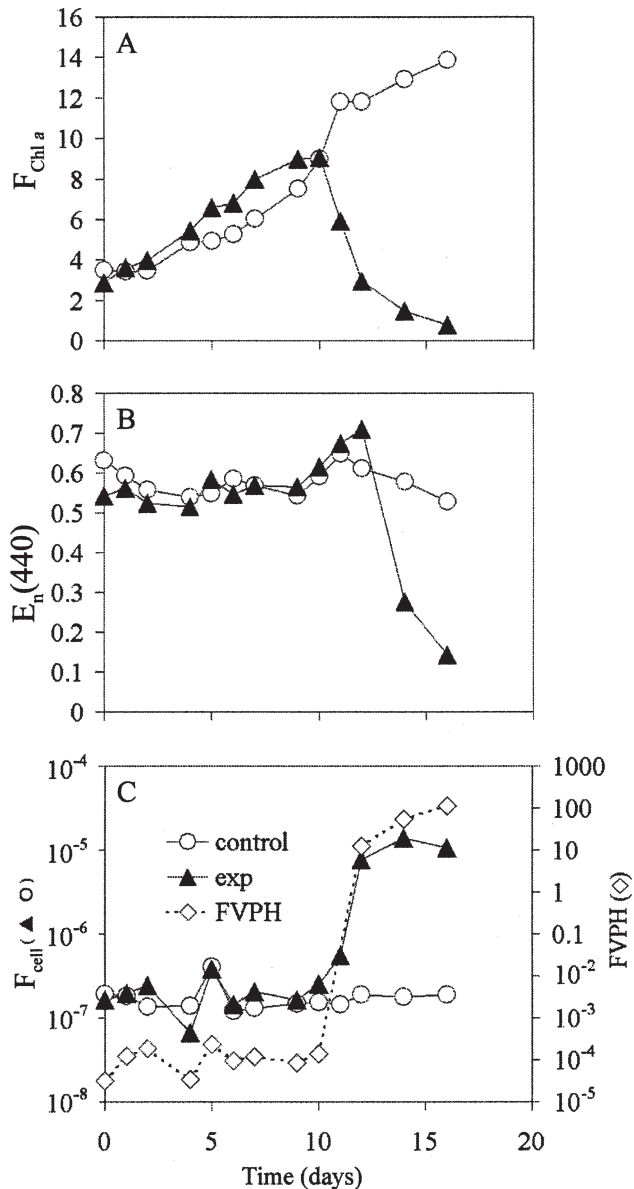


Fig. 7. (A) Bulk Chl *a* fluorescence ($F_{Chl\ a}$; relative scale) of host *Synechococcus* strain 1334 cells during viral infection experiment (same experiment as in Fig. 1). (B) Chlorophyll fluorescence efficiency, $E_n(440)$ ($=F_{Chl\ a}/a_{pg}(440)$) over course of experiment. (C) Plot of chlorophyll fluorescence per cell (F_{cell}) over duration of infection experiment with *Synechococcus* strain 1334 (same experiment as in Fig. 1). Also shown is the time course of the ratio of free viruses per host cell (FVPH given on second y-axis). All symbols as in key in (C).

fluorescence and absorption roughly followed the same trajectory (slope) through day 10, after which the infected cells showed slightly higher fluorescence efficiency from days 10–12 as hosts were lysed and both absorption and fluorescence decreased in tandem. It was not until days 14 and 16 that the fluorescence and absorption trends markedly deviated from the trends seen during earlier growth.

The above observations were consistent with the hypothesis that, early on, the photophysiology of the

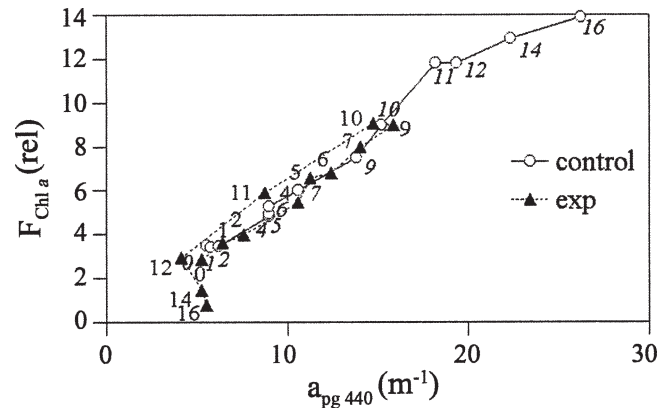


Fig. 8. Chl *a* fluorescence, $F_{Chl\ a}$ (relative) versus $a_{pg}(400)$ (m^{-1}) during infection experiment with *Synechococcus* strain 1334 (same experiment as in Fig. 1). Numbers besides symbols represent the number of days after infection. Italic numerals refer to control samples; nonitalic numerals represent time course of infected cells.

Synechococcus was unchanged by infection and slight increases in $F_{Chl\ a}$ values of infected flasks (Fig. 7A) were because these cells synthesized more pigment per cell. Moreover, trends in the FVPH and F_{cell} in the experimental flask were almost identical, suggesting a link between them (note, however, that changes in F_{cell} spanned almost four orders of magnitude, and changes in FVPH spanned almost seven orders of magnitude).

Although there were subtle increases in F_{cell} during early infection, the decrease in fluorescence after lysis was much more pronounced. Indeed, the radical reduction in bulk fluorescence was associated with the near-complete (~99%) lysis of the host cells (Fig. 1). The relationship between FVPH and F_{cell} fit a power law in which F_{cell} changed as the cube root of the FVPH ($F_{cell} = 3.3 \times 10^{-6} (FVPH)^{0.313}$; $r^2 = 0.98$; $n = 11$; $p < 0.001$). The high correlation statistics should be interpreted cautiously, however, because the data are not normally distributed but instead showed a bimodal distribution (Fig. 9). Nonetheless, this figure demonstrates that changes in F_{cell} , as well as FVPH, were so rapid that our daily sampling only captured early and late stages of infection, and perhaps not the intermediate ones.

One hypothesis for the above observations is that the increase in cellular fluorescence during the late stages of infection resulted from the physiological disconnect between the light reactions of photosynthesis and electron transport into the dark reactions of photosynthesis in a manner similar to the effect of the photosynthetic inhibitor DCMU (3-(3,4-dichlorophenyl)-1,1-dimethylurea) (Vincent 1980). Moreover, after host lysis, some host regrowth was observed, suggesting that these cells were virus resistant. If true, then the infection selected for virus-resistant host cells over the timescale of our experiments, which is consistent with the observations of Waterbury and Valois (1993). In addition, it is noteworthy that these virus-resistant host cells were almost always slower growing than the nonresistant cells. An alternative hypothesis is that this was not true host resistance but that in the late stages of infection, there were high concentrations of defective

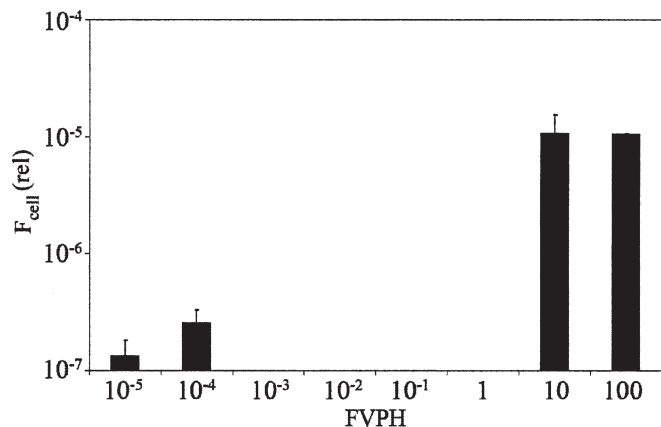


Fig. 9. Histogram of Chl *a* fluorescence per cell (F_{cell} ; relative scale) versus free viruses per host cell (FVPH) for infected *Synechococcus* strain 1334 (same experiment as in Fig. 1). The major virus burst occurred between samplings on days 10 and 11; hence, there are two well-defined groups of data points. Results suggest that cellular fluorescence increased as approximately the cube root of the FVPH (see text).

viruses that blocked host receptor sites from infective viruses. This conceivably could have slowed the rate of infection by functional viruses, thus slowing the net growth rate.

The shift in absorption from well-defined pigment absorption peaks across the visible spectrum to blue-dominated absorption after infection was also striking (Figs. 5 and 6). Postinfection absorption spectra resembled the absorption spectra of phytoplankton detritus, with decreasing absorption from blue to red wavelengths, along with chromophoric dissolved organic matter, gelbstoff, which has a log-linear decrease in absorption from the UV into blue wavelengths (Roesler and Perry 1989). These observations are fully consistent with the interpretation that after infection, the optical properties were driven by a combination of *Synechococcus* debris (with loss of pigment absorption and increase in backscattering) and release of chromophoric dissolved organic matter during lysis. This view is consistent with the notion that viruses are important agents in termination of blooms and in the conversion of the particulate organic matter to dissolved organic matter (Bratbak et al. 1990).

Strong decreases in backscattering also are consistent with the loss of turbidity reported by others after *Synechococcus* infection by viruses (Wilson et al. 1996; Balch et al. 2002). The rate of decrease in backscattering was usually not the same as the decrease in absorption, however (Table 3), so an obvious question arises. What is the optical effect of viral infection on the reflectance of a cyanobacterial bloom? This is an intriguing question because reflectance at a given wavelength is inversely proportional to the absorption, and because it increases with increases in backscattering in a curvilinear saturating fashion (Gordon et al. 1988).

The answer to the question of viral effects on reflectance is beyond the scope of this article but would be highly relevant to the observation of virus-infected phytoplankton blooms by means of satellite remote sensing. Dense

Synechococcus blooms have been documented in the field before (Morel 1997). Moreover, there are numerous accounts of the demise of other types of phytoplankton blooms (e.g., coccolithophores) that appeared to be mediated by viruses (Wilson et al. 2002). It thus seems reasonable that naturally occurring *Synechococcus* blooms also could be virally controlled. If viral infection of a field bloom causes similar changes in inherent optical properties comparable to what we observed in our laboratory experiments, there almost certainly would be changes in remote sensing reflectance. This especially would seem likely given the recent results of Simis et al. (2005), in which the virus-induced lysis of a bloom of a fresh water filamentous cyanobacterial species, *Limnothrix* sp., was associated with changes in the remote sensing reflectance. The exact magnitude of any reflectance changes associated with an infected *Synechococcus* bloom (and whether they are detectable by remote sensing) will have to await further observation and modeling studies.

References

- BABIN, M., AND D. STRAMSKI. 2002. Light absorption by aquatic particles in the near-infrared spectral region. *Limnol. Oceanogr.* **47**: 911–915.
- BALCH, W. M., AND D. T. DRAPEAU. 2004. Backscattering by coccolithophorids and coccoliths: Sample preparation, measurement and analysis protocols, p. 27–36. *In* J. L. Mueller, G. S. Fargion and C. R. McClain [eds.], *Ocean optics protocols for satellite ocean color sensor validation, revision 5: Biogeochemical and bio-optical measurements and data analysis protocols*. National Aeronautical and Space administration, Goddard Space Flight Space Center.
- , T. L. CUCCI, R. D. VAILLANCOURT, K. A. KILPATRICK, AND J. J. FRITZ. 1999. Optical backscattering by calcifying algae—separating the contribution by particulate inorganic and organic carbon fractions. *J. Geophys. Res.* **104**: 1541–1558.
- , J. M. VAUGHN, J. F. NOVOTNY, D. T. DRAPEAU, J. I. GOES, J. M. LAPIERRE, E. SCALLY, C. L. VINING, A. ASHE, AND J. M. J. VAUGHN. 2002. Fundamental changes in light scattering associated with infection of marine bacteria by bacteriophage. *Limnol. Oceanogr.* **47**: 1554–1561.
- , ———, ———, ———, R. D. VAILLANCOURT, J. LAPIERRE, AND A. ASHE. 2000. Light scattering by viral suspensions. *Limnol. Oceanogr.* **45**: 492–498.
- BEARDSLEY, G. F., AND J. R. V. ZANEVELD. 1969. Theoretical dependence of the near-asymptotic apparent optical properties on the inherent optical properties of sea water. *J. Opt. Soc. Am.* **59**: 373–377.
- BERGH, O., K. Y. BOERSHEIM, G. BRATBAK, AND M. HELDAL. 1989. High abundance of viruses found in aquatic environments. *Nature* **340**: 467–468.
- BETTAREL, Y., AND OTHERS. 2002. Strong, weak, and missing links in a microbial community of the N.W. Mediterranean Sea. *FEMS Microbiol. Ecol.* **42**: 451–462.
- BRATBAK, G., M. HELDAL, S. NORLAND, AND T. F. THINGSTAD. 1990. Viruses as partners in spring bloom microbial trophodynamics. *Appl. Environ. Microbiol.* **56**: 1400–1405.
- BRICAUD, A., AND D. STRAMSKI. 1990. Spectral absorption coefficients of living phytoplankton and nonalgal biogenous matter: A comparison between the Peru upwelling area and the Sargasso Sea. *Limnol. Oceanogr.* **35**: 562–582.

- CHIN, W. C., M. V. ORELLANA, AND P. VERDUGO. 1998. Spontaneous assembly of marine dissolved organic matter into polymer gels. *Nature* **391**: 568–572.
- CLEVELAND, J. S., AND M. J. PERRY. 1994. A model for partitioning particulate absorption into phytoplankton and detrital components. *Deep-Sea Res. I* **41**: 197–221.
- COTTRELL, M. T., AND C. A. SUTTLE. 1991. Wide-spread occurrence and clonal variation in viruses which cause lysis of a cosmopolitan, eukaryotic marine phytoplankter, *Micromonas pusilla*. *Mar. Ecol. Progr. Ser.* **78**: 1–9.
- GOERCKE, R., AND N. A. WELSCHMEYER. 1993. The marine prochlorophyte *Prochlorococcus* contributes significantly to phytoplankton biomass and primary production in the Sargasso Sea. *Deep-Sea Res. I* **40**: 11–12.
- GORDON, H. 1976. Radiative transfer in the ocean: A method for determination of absorption and scattering properties. *Appl. Opt.* **15**: 2611–2613.
- GORDON, H. R., O. B. BROWN, R. H. EVANS, J. W. BROWN, R. C. SMITH, K. S. BAKER, AND D. K. CLARK. 1988. A semianalytic radiance model of ocean color. *J. Geophys. Res.* **93**: 10909–10924.
- HEWSON, I., J. M. O'NEIL, C. A. HEIL, G. BRATBAK, AND W. C. DENNISON. 2001. Effects of concentrated viral communities on photosynthesis and community composition of cooccurring benthic microalgae and phytoplankton. *Aquat. Microb. Ecol.* **25**: 1–10.
- JUNEAU, P., J. E. LAWRENCE, C. A. SUTTLE, AND P. J. HARRISON. 2003. Effects of viral infection on photosynthetic processes in the bloom-forming alga *Heterosigma akashiwo*. *Aquat. Microb. Ecol.* **31**: 9–17.
- KIRK, J. T. O. 1994. Light and photosynthesis in aquatic ecosystems, 2nd ed. Cambridge Univ. Press.
- MCDANIEL, L., L. A. HOUCHEIN, S. J. WILLIAMSON, AND J. H. PAUL. 2002. Plankton blooms: Lysogeny in marine *Synechococcus*. *Nature* **415**: 496.
- MOBLEY, C. D. 1994. Light and water: Radiative transfer in natural waters. Academic Press.
- MOREL, A. 1997. Consequences of a *Synechococcus* bloom upon the optical properties of oceanic (case 1) waters. *Limnol. Oceanogr.* **42**: 1746–1754.
- , AND Y. AHN. 1990. Optical efficiency factors of free-living marine bacteria: Influence of bacterioplankton upon the optical properties and particulate organic carbon in oceanic waters. *J. Mar. Res.* **48**: 145–175.
- , AND ———. 1991. Optics of heterotrophic nanoflagellates and ciliates: A tentative assessment of their scattering role in oceanic waters compared to those of bacterial and algal cells. *J. Mar. Res.* **49**: 177–202.
- NOBLE, R. T., AND J. A. FUHRMAN. 1998. Use of SYBR Green I for rapid epifluorescence counts of marine viruses and bacteria. *Aquat. Microb. Ecol.* **14**: 113–118.
- OGURA, N., AND T. HANYA. 1967. UV absorption of the seawater in relation to organic and inorganic matter. *Int. J. Oceanol. Limnol.* **1**: 91–102.
- ONG, L. J., AND A. N. GLAZER. 1991. Phycoerythrins of marine unicellular Cyanobacteria. 1. Bilin types and locations and energy transfer pathways in *Synechococcus* spp. phycoerythrins. *J. Biol. Chem.* **266**: 9515–9527.
- PALENIK, B., AND OTHERS. 2003. The genome of a motile marine *Synechococcus*. *Nature* **424**: 1037–1042.
- PAUL, J. H., S. C. JIANG, AND J. B. ROSE. 1991. Concentration of viruses and dissolved DNA from aquatic environments by vortex flow filtration. *Appl. Environ. Microbiol.* **57**: 2197–2204.
- PETZOLD, T. J. 1972. Volume scattering functions for selected ocean waters, p. 72–78. University of California Scripps Institute of Oceanography.
- ROESLER, C. S., AND M. J. PERRY. 1989. Modeling in situ phytoplankton absorption from total absorption spectra in productive inland marine waters. *Limnol. Oceanogr.* **34**: 1510–1523.
- ROHOZINSKI, J., P. N. PATIL, AND G. G. R. SEATON. 1995. Infectivity of algal viruses studied by chlorophyll fluorescence. *J. Gen. Virol.* **76**: 2859–2862.
- SEATON, G. G. R., K. LEE, AND J. ROHOZINSKI. 1995. Photosynthetic shutdown in *Chlorella* NC64A associated with the infection cycle of the virus PBCV-1. *Plant Physiol.* **108**: 1431–1438.
- SIMIS, S. G. H., M. TIJDENS, H. L. HOOGVELD, AND H. J. GONS. 2005. Optical changes associated with cyanobacterial bloom termination by viral lysis. *J. Plankton Res.* **27**: 937–949.
- STRAMSKI, D., AND D. A. KIEFER. 1991. Light scattering by microorganisms in the open ocean. *Progr. Oceanogr.* **28**: 343–383.
- SUTTLE, C. A., AND A. M. CHAN. 1993. Marine cyanophages infecting oceanic and coastal strains of *Synechococcus*: Abundance, morphology, cross-infectivity and growth characteristics. *Mar. Ecol. Progr. Ser.* **92**: 99–109.
- , AND ———. 1994. Dynamics and distribution of cyanophages and their effect on marine *Synechococcus* spp. *Appl. Environ. Microbiol.* **60**: 3167–3174.
- TOLEDO, G., B. PALENIK, AND B. BRAHAMSHA. 1999. Swimming marine *Synechococcus* strains with widely different photosynthetic pigment ratios form a monophyletic group. *Appl. Environ. Microbiol.* **65**: 5247–5251.
- TWARDOWSKI, M. S., E. BOSS, J. B. MACDONALD, W. S. PEGAU, A. H. BARNARD, AND J. R. V. ZANEVELD. 2001. A model for estimating bulk refractive index from the optical backscattering ratio and the implications for understanding particle composition in case I and case II waters. *J. Geophys. Res. C Oceans* **106**: 129–114.
- VAILLANCOURT, R. D., AND W. M. BALCH. 2000. Size distribution of coastal sub-micron particles determined by flow, field flow fractionation. *Limnol. Oceanogr.* **45**: 485–492.
- VINCENT, W. F. 1980. Mechanisms of rapid photosynthetic adaptation in natural phytoplankton communities. II. Changes in photochemical capacity as measured by DCMU-induced chlorophyll fluorescence. *J. Phycol.* **16**: 568–577.
- WATERBURY, J. B., AND F. W. VALOIS. 1993. Resistance to co-occurring phages enables marine *Synechococcus* communities to coexist with cyanophages abundant in seawater. *Appl. Environ. Microbiol.* **59**: 3393–3399.
- WILSON, W. H., N. G. CARR, AND N. H. MANN. 1996. The effect of phosphate status on the kinetics of cyanophage infection in the oceanic cyanobacterium *Synechococcus* sp. WH7803. *J. Phycol.* **32**: 506–516.
- , I. R. JOINT, N. G. CARR, AND N. H. MANN. 1993. Isolation and molecular characterization of five marine cyanophages propagated on *Synechococcus* sp. strain WH7803. *Appl. Environ. Microbiol.* **59**: 3736–3743.
- , G. A. TARRAN, D. SCHROEDER, M. COX, J. OKE, AND G. MALIN. 2002. Isolation of viruses responsible for the demise of an *Emiliania huxleyi* bloom in the English Channel. *J. Mar. Biol. Assn. UK* **82**: 369–377.
- WOOD, A. M., D. A. PHINNEY, AND C. S. YENTSCH. 1998. Water column transparency and the distribution of spectrally distinct forms of phycoerythrin-containing organisms. *Mar. Ecol. Progr. Ser.* **162**: 25–31.

Received: 2 March 2006

Accepted: 12 September 2006

Amended: 23 October 2006